excursions characterizing the boundary horizon (*21*) may be explained otherwise; a rapid and abundant input of fossilized light carbon into the atmospheric and oceanic circulation systems (*1*, *4*) is possible.

REFERENCES AND NOTES

1. J. J. Sepkoski Jr., *J. Geol. Soc. London* **146**, 7 (1984); D. H. Erwin, *The Great Paleozoic Crisis* (Columbia Univ. Press, New York, 1993); *Nature* **367**, 231 (1994).
2. A. H. Knoll, R. K. Bambach, D. E. Canfield, J. P. Grotzinger, *Science* **273**, 452 (1996); J. P. Grotzinger and A. H. Knoll, *Palaios* **10**, 578 (1995).
3. S. Yamakita, *J. Geol. Soc. Jpn.* **93**, 145 (1987).
4. Y. Isozaki, *Can. Soc. Petrol. Geol. Mem.* **17**, 805 (1994).
5. Absence of carbonate and coarse-grained terrigenous grains indicates that the primary depositional site was deeper than the carbonate compensation depth (CCD) of ~4000 m and was remote from land areas. [T. Matsuda and Y. Isozaki, *Tectonics* **10**, 475 (1991); Y. Isozaki, *Island Arc* **5**, 289 (1996); *ibid.* **6**, 28 (1997)].
6. C. Scotese and R. P. Langford, in *Paleogeography, Paleoclimates, Stratigraphy*, vol. 1 of *The Permian of Northern Pangea*, P. A. Scholle, T. M. Peryt, D. S. Ulmer-Scholle, Eds. (Springer-Verlag, Berlin, 1995), pp. 3–19.
7. K. Nakao and Y. Isozaki, *J. Geol. Soc. Jpn.* **100**, 505 (1994); K. Kubo, Y. Isozaki, M. Matsuo, *ibid.* **102**, 40 (1996).
8. Y. Kajiwara *et al.*, *Palaeogeogr. Palaeoclimatol. Palaeoecol.* **111**, 367 (1994); Y. Kakuwa, *ibid.* **121**, 35 (1996); H. Ishiga, K. Ishida, K. Dozen, M. Musashino, *Island Arc* **5**, 180 (1996).
9. Age assignment of the PTBU is based on conodont biostratigraphy. The youngest Permian conodonts occur from the lower siliceous claystone. They are poorly preserved but morphologically resemble *Gondolella changxingensis* (Wang), an index species for the Changxingian stage, latest Permian. The oldest Triassic conodonts are from the upper siliceous claystone and include *Neospathodus dieneri* (Sweet), *N. waageni* (Sweet), and *N. conservativus* (Müller) that indicate the Dienerian to Spathian, Early Triassic. Although no index fossil indicating the Changxingian or Griesbachian stage has been obtained, the boundary is assigned in the carbonaceous claystone. Late Permian and Early Triassic radiolarian faunas from adjacent cherts are consistent with this age assignment. See S. Yamakita, 1993 Annual Meeting of the Geological Society of Japan, Abstracts with Program, p. 65; K. Sugiyama, *Trans. Proc. Paleont. Soc. Jpn.* **167**, 1180 (1992); K. Kuwahara, S. Nakae, A. Yao, *J. Geol. Soc. Jpn.* **97**, 1005 (1993); (*3*, *4*). The timescale used here is after C. Ross, A. Baud, and M. Menning [*Can. Soc. Petrol. Geol. Mem.* **17**, 81 (1994)]. Concerning the relevant Permo-Triassic interval, chronology of stage boundaries is not well constrained except for two tie-points, that is, 251 million years ago at the P-T boundary and 234 million years ago at the Anisian-Ladinian boundary.
10. Y. Isozaki *et al.*, in *Geology and Paleontology of Japan and East Asia*, H. Noda and K. Sashida, Eds. (Gakujutu Tosho, Tokyo, 1996), pp. 245–251. For the Permian and Middle to Late Triassic cherts, see F. Cordey [*Curr. Res. Geol. Surv. Can.* **86-1A**, 595 (1986)] and M. Orchard [*ibid.*, **84-1B**, 197 (1984)].
11. The Permo-Triassic chert sections with the PTBU occur in the Jurassic accretionary complex for nearly 1000 km along the Japanese islands from north of Tokyo to Kyushu island (*3*), which suggests that its primary distribution was more extensive.
12. The deep-sea anoxia started in the *Follicucullus scholasticus* (radiolarian) zone that indicates the latest Guadalupian to earliest Wuchapingian, and it ended in the *Eptingium manfredi*–group (radiolarian) zone of the mid-Anisian. According to the timescale (*9*), this interval is estimated to be nearly 20 My.
13. The well-known Cenomanian-Turonian (Cretaceous) anoxia is no longer than 1 to 2 My and others are much shorter [H. C. Jenkyns, *J. Geol. Soc. London* **137**, 171 (1980); *Am. J. Sci.* **288**, 101 (1988); W. W. Hay, *Geol. Soc. Am. Bull.* **100**, 1934 (1988)].
14. Most modern radiolarians live in the surface water of oceans, particularly in the photic zone because they engage in symbiosis with photosynthetic algae. Their skeletal remains fall through the water column and accumulate on the deep seafloor below the CCD.
15. W. S. Broecker and G. H. Denton, *Geochim. Cosmochim. Acta* **53**, 2465 (1989).
16. R. V. Tyson, R. C. L. Wilson, C. Downie, *Nature* **277**, 377 (1979).
17. P. Wignall and A. Hallam, *Palaeogeogr. Palaeoclimatol. Palaeoecol.* **93**, 21 (1992); *ibid.* **102**, 215 (1993); A. Hallam, *Can. Soc. Petrol. Geol. Mem.* **17**, 797 (1994); P. Wignall and R. J. Twitchett, *Science* **272**, 1155 (1996).
18. S. M. Stanley and X. Yang, *Science* **266**, 1340 (1994).
19. E. Flügel, *Geol. Soc. Am. Spec. Pap.* **288**, 247 (1994).
20. J. J. Sepkoski Jr., in *Global Bio-Events*, O. Walliser, Ed. (Springer-Verlag, Berlin, 1986), pp. 47–61.
21. M. Magaritz and K. H. Schulze, *Contrib. Sedimentol.* **9**, 269 (1980); K. Malkowski, M. Gruszynski, A. Hoffman, S. Hallas, *Hist. Biol.* **2**, 289 (1989); A. Baud, M. Magaritz, W. Holser, *Geol. Rundsch.* **78**, 649 (1989); W. Holser *et al.*, *Nature* **337**, 39 (1989).
22. K. Sugiyama, 1995 Annual Meeting of the Paleontological Society of Japan, Abstracts with Program, p. 124; H. Ishiga, in *Pre-Cretaceous Terranes of Japan*, K. Ichikawa, S. Mizutani, I. Hara, S. Hada, A. Yao, Eds. (Nippon Insatsu, Osaka, Japan, 1990), pp. 285–295.
23. P. F. Hoffman and J. M. Edmond critically reviewed an early version of the manuscript. W. R. Danner, F. Cordey, M. Orchard, T. Koike, and H. Sano provided valuable information of the Cache Creek cherts. Supported by the Ministry of Culture and Education of Japan (Intensified Study Area Program number 259, 1995 through 1997).

21 October 1996; accepted 3 February 1997

Ferroelectric Field Effect Transistor Based on Epitaxial Perovskite Heterostructures

S. Mathews, R. Ramesh, T. Venkatesan, J. Benedetto

Ferroelectric field effect devices offer the possibility of nonvolatile active memory elements. Doped rare-earth manganates, which are usually associated with colossal magnetoresistive properties, have been used as the semiconductor channel material of a prototypical epitaxial field effect device. The carrier concentration of the semiconductor channel can be "tuned" by varying the manganate stochiometry. A device with $La_{0.7}Ca_{0.3}MnO_3$ as the semiconductor and $PbZr_{0.2}Ti_{0.8}O_3$ as the ferroelectric gate exhibited a modulation in channel conductance of at least a factor of 3 and a retention loss of 3 percent after 45 minutes without power.

The remanent polarization of ferroelectric thin films offers the possibility of nonvolatile memory elements (*1*). For example, the ferroelectric field effect transistor (FET) (*2*) permits a nondestructive memory readout because the device can be interrogated by reading the conductance of the semiconductor channel. Unlike ferroelectric capacitive memory elements, the act of reading does not affect the state of the device.

Recently, doped rare-earth manganates such as $La_{1-x}Ca_xMnO_3$ (LCMO) have stirred considerable excitement due to the observation of very large magnetoresistance in these materials (*3*). These manganates show a "metal-semiconductor" transition as a function of temperature. A measurable, although anomalous, field effect has been seen in these semiconducting colossal magnetoresistance (CMR) manganate materials (*4*). These materials are perovskites and are closely lattice-matched to the common perovskite ferroelectrics; thus, they present an interesting opportunity to create field effect devices that may potentially be both electrically and magnetically tuned.

Although ferroelectric FETs have been studied since the 1950s (*5*), an acceptable nonvolatile, nondestructive read memory with adequate retention and write-erase speed has yet to be demonstrated (*2*), mainly because the interface between the perovskite ferroelectric and a semiconductor such as silicon is quite difficult to control. Any imperfections at the interface, such as the formation of undesirable phases or electronic trapping states, will seriously degrade the performance of the device. The use of an epitaxial perovskite heterostructure has therefore been proposed as a way of improving the interface quality.

The carrier concentration of the LCMO semiconductor varies widely with both the Ca:Mn ratio and oxygen stochiometry, and so the semiconductor channel can be "tuned" to the ferroelectric gate. The ferroelectric induces a charge per unit area in the semiconductor equal to the spontaneous polarization of the ferroelectric. In order

---

S. Mathews, Department of Materials and Nuclear Engineering, University of Maryland, College Park, MD 20742, USA.
R. Ramesh, Department of Materials and Nuclear Engineering and Center for Superconductivity Research, University of Maryland, College Park, MD 20742, USA.
T. Venkatesan, Center for Superconductivity Research, University of Maryland, College Park, MD 20742, USA.
J. Benedetto, Army Research Laboratory, Adelphi, MD 20783–1197, USA.

to achieve large values of modulation, the number of carriers in the semiconductor should not be large with respect to the amount of available charge induced by the ferroelectric (6). For a given channel modulation and a fixed carrier mobility, the spontaneous polarization of the ferroelectric determines the carrier concentration and therefore the conductivity range of the semiconductor to be used. A high "off-state" resistance and a low "on-state" resistance therefore become competing factors. Varying the channel carrier concentration allows one to strike an appropriate balance between these two competing performance characteristics.

Several researchers have recently reported on the fabrication and testing of all perovskite ferroelectric field effect devices. In 1994, Watanabe reported on a device in which $La_{2-x}Sr_xCuO_4$ was used as the semiconductor channel (7), which showed a maximum modulation of 9.5%. With a lower modulation (~5%), this device exhibited retention at room temperature over periods of several days. In 1995, Ahn *et al.* reported on a device in which $SrCuO_2$ was used as a semiconductor (6) with ~3.5% modulation. Retention on this device was measured only to 10 min, at which point no change in channel resistance was observed. Some researchers, in particular Ogale *et al.* (4), have questioned whether the observed change in the transport properties of the oxide semiconductor is a field effect or occurs by some other mechanism. We note that neither Watanabe nor Ahn directly observed accumulation-depletion behavior indicative of a field effect in the devices.

We report an all-perovskite ferroelectric field effect device made of a CMR material that shows at least 300% modulation with retention at least on the order of several hours. Our capacitance versus voltage data are consistent with the formation of accumulation and depletion regions in the oxide semiconductor. Thin films were grown on (001)-oriented, single-crystal $LaAlO_3$ substrates by pulsed laser deposition (8, 9). For a poling voltage of 7 V, our ferroelectric hysteresis loops (Fig. 1) were relatively "square," and the remnant polarization values, 35 to 40 μC/cm², were quite high (10).

To test the electrical properties of the device, we ran a trickle current of 1.0 to 1000 μA from drain to source and intermittently applied a voltage source to the ferroelectric gate (Fig. 2). After the gate voltage was removed, the voltage drop across the channel (V_{SD}) was measured. The source-drain voltage was measured 2 to 3 s after the gate voltage was turned off to allow any switching transients to die down. All measurements were performed at room temperature. Figure 3 shows a hysteresis loop obtained by measuring the channel resistance of a device as a function of the poling voltage. As described above, the gate is actually floating when the channel resistance *R* is measured. This device showed channel modulation of approximately 3 $[(R_{max} - R_{min})/R_{min}]$. As FETs, these devices show relatively low modulation and high on-state resistance, but the on/off ratio is comparable to that of dynamic random access memory (DRAM) (5), and the channel resistance is not prohibitively high for such applications.

In order to verify that the channel modulation observed in Fig. 3 can plausibly be attributed to a field effect, we consider the following argument. The LCMO channel is a *p*-type material, so the majority of carriers in the channel are holes. The application of a positive voltage to the gate polarizes the ferroelectric such that the electric dipole moments point down, into the semiconductor. This rearrangement effectively causes the buildup of a positive charge on the bottom side of the ferroelectric that will tend to be compensated by negative carriers in the channel, thereby depleting the channel of positive holes. We therefore would expect the channel resistance to increase

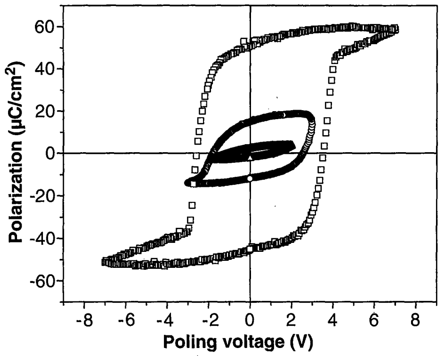

Fig. 1. Ferroelectric hysteresis loops for a $La_{1-x}Sr_xCoO_3$/LCMO/PZT/Pt stack. These loops from one sample are characteristic of those observed for all samples in this study. PZT, lead ziconate titanate.

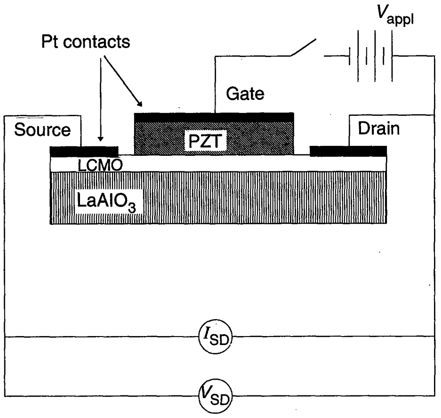

Fig. 2. Schematic diagram of an all-perovskite ferroelectric FET and measurement circuit.

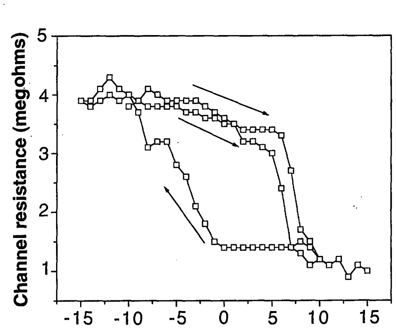

Fig. 3. Channel resistance hysteresis loop for an all-perovskite ferroelectric FET. Channel resistance is measured with the gate floating. Note that the counterclockwise direction of the loop indicates ferroelectric switching.

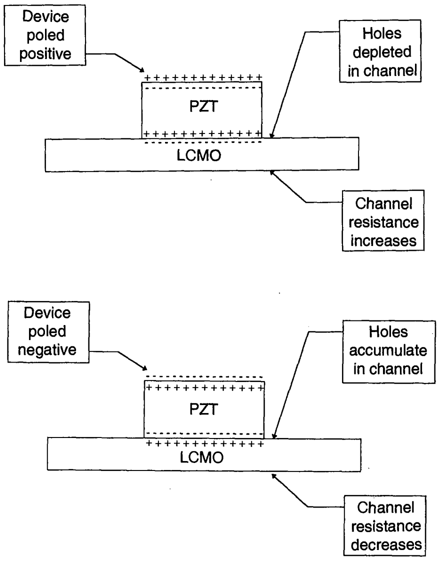

Fig. 4. Schematic diagram of a simplified model for the field effect in a *p*-type ferroelectric FET.

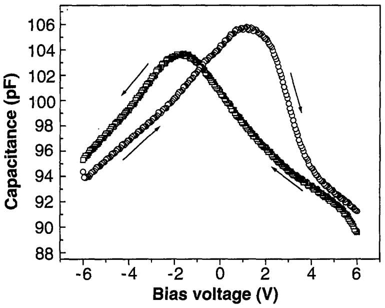

Fig. 5. Capacitance-voltage curves for a Pt/PZT/LCMO capacitor. Note the decrease in capacitance under positive bias, consistent with the formation of a depletion region in the semiconductor. Also note the direction of the arrows, indicating ferroelectric switching, rather than charge injection.

when the ferroelectric is poled positive (Fig. 4A) and to decrease when it is poled negative (Fig. 4B). The device clearly behaves (Fig. 3) as one would expect if the channel modulation was the result of a field effect.

We measured no change in channel resistance after shorting the top and bottom electrodes through a 1-megohm resistor. We measured only a 3% change in the channel resistance after waiting 45 min at room temperature. Capacitance verses bias voltage curves for a PZT/LCMO capacitor (PZT, lead zirconate titanate) grown under the same conditions as the FET devices (Fig. 5) show ferroelectric switching rather than charge injection. The higher capacitance at negative bias voltage, as compared to positive bias voltage, is consistent with the formation of a depletion layer in a *p*-type semiconductor. These observations indicate that the channel modulation is in fact caused by a field effect and not "charge-up" or charge injection.

The present results demonstrate that a markedly improved, nonvolatile ferroelectric field effect device can be constructed of perovskite heterostructures with a magnetoresistive manganate as the channel semiconductor. The enhanced interface characteristics associated with the ferroelectric-manganate interface allows for the fabrication of field effect devices with channel-resistance modulation of at least a factor of 3 and retention on the order of hours.

REFERENCES AND NOTES

1. R. Ramesh *et al.*, *Appl. Phys. Lett.* **64**, 1588 (1994).
2. P. M. Heyman and G. H. Heilmeier, *Proc. IEEE* **54**, 842 (1966).
3. S. Jin *et al.*, *Science* **264**, 413 (1994).
4. S. B. Ogale *et al.*, *Phys. Rev. Lett.* **77**, 1159 (1996).
5. D. H. Looney, U.S. Patent 2 791 758 (1957); W. L. Brown, U.S. Patent 2 791 759 (1957); I. M. Ross, U.S. Patent 2 791 760 (1957); J. A. Morton, U.S. Patent 2 791 761 (1957).
6. C. H. Ahn *et al.*, *Science* **269**, 373 (1995).
7. Y. Watanabe, *Appl. Phys. Lett.* **66**, 1770 (1995).
8. R. Ramesh *et al.*, *Science* **252**, 944 (1991).
9. The ferroelectric layers were patterned by in situ mechanical masking. The semiconductor channel and electrodes were patterned with photolithographic wet etch and lift-off techniques, respectively. Samples were then photolithographically patterned again and ion-milled in order to isolate individual devices. The perovskite semiconductor layer, LCMO, was between 300 to 500 Å thick. The ferroelectric layer, PZT, was between 3000 and 4000 Å in thickness. Platinum electrodes, 1000 Å in thickness, were deposited ex situ after the patterning of the other layers. Analysis by x-ray diffraction, performed before patterning and electrode deposition, indicated that no undesirable phases were formed and that both the LCMO and PZT were well-oriented with strong [001] texture. Rutherford backscattering data confirmed that the film stochiometry was consistent (within error) with that of the target materials. Transmission electron microscopy showed that the interfaces were sharp and smooth with no significant interdiffusion or formation of secondary phases. Pulsed hysteresis loops were acquired at room temperature with a Radiant Technologies RT-66A measurement system in order to determine the ferroelectric properties of the PZT layer.
10. The hysteresis loops in Figs. 1 and 3 are shifted slightly toward negative gate voltages. We attribute this shift to the fact that the top and bottom electrodes are made of different materials. Because the carrier concentration and electronic work function of the top and bottom electrodes are different, we expect this type of asymmetry in the hysteresis of the devices.
11. S.M. and R.R. would like to acknowledge the support of the U.S. Department of Army Federated Laboratories. T.V. would like to acknowledge the support of NSF grant DMR 9404579.

26 August 1996; accepted 12 February 1997

Melting Temperature and Partial Melt Chemistry of H_2O-Saturated Mantle Peridotite to 11 Gigapascals

Tatsuhiko Kawamoto and John R. Holloway*

The H_2O-saturated solidus of a model mantle composition (Kilborne Hole peridotite nodule, KLB-1) was determined to be just above 1000°C from 5 to 11 gigapascals. Given reasonable H_2O abundances in Earth's mantle, an H_2O-rich fluid could exist only in a region defined by the wet solidus and thermal stability limits of hydrous minerals, at depths between 90 and 330 kilometers. The experimental partial melts monotonously became more mafic with increasing pressure from andesitic composition at 1 gigapascal to more mafic than the starting peridotite at 10 gigapascals. Because the chemistry of the experimental partial melts is similar to that of kimberlites, it is suggested that kimberlites may be derived by low-temperature melting of an H_2O-rich mantle at depths of 150 to 300 kilometers.

H_2O lowers melting temperatures of mantle peridotites and also affects the chemistry of their partial melts (*1*, *2*). Earlier experiments demonstrated that partial melting of H_2O-saturated peridotite produces andesitic or dacitic melts at 1 GPa, in contrast to basaltic melts in dry peridotite (*2*). Therefore, it was surprising that partial melting of H_2O-saturated peridotites at pressures greater than 5 GPa produced ultramafic melts (*3*, *4*). Two ultramafic magma types are known on Earth: komatiites and kimberlites. Komatiites are believed to represent high-temperature melts in the early Earth. However, recent experiments (*3*, *4*) led to suggestions that komatiites could be produced by wet peridotite melting (*3*–*5*), and hence they could shed light on the degassing history of Earth's mantle (*6*). Kimberlites contain diamonds and peridotite nodules that are the only samples from the mantle's deepest depths (~150 to 200 km). Understanding the origin of these ultramafic magmas would provide important clues to the evolution of Earth's mantle.

In an effort to understand the effect of H_2O on the generation of ultramafic magmas, we undertook a precise determination of solidus temperatures and partial melt chemistry in an H_2O-saturated peridotite. The starting material was a mixture of an Mg-free KLB-1 peridotite gel and brucite, resulting in molar ratios of 89 for Mg/(Mg + Fe) × 100 (Mg#) and 1.46 for (Mg + Fe)/Si, with an H_2O content of 13.7% (by weight). The chemistry of KLB-1 peridotite is similar to that of pyrolite mantle (*7*). The ground starting material was put in a thick-walled Ag capsule with a few pieces of folded Ag foil (0.05 mm thick) (Fig. 1A). The foil was used to extract partial melts by capillary action (*8*). This sample assembly was placed inside a box-shaped graphite furnace. We used Ag to minimize Fe loss to the capsule and maximize thermal conductivity. The temperature was monitored by an S-type thermocouple placed at the top of the sample assembly, and the thermal gradient along the sample (0.5 mm long) was estimated to be <50°C (*9*). We heated samples to temperatures from 950° to 1100°C at pressures from 5 to 11 GPa (Table 1).

We determined the solidus temperature by observing the dendritic texture of quenched partial melts associated with the Ag foils (Fig. 1B) and the increase in the Mg# of olivine crystals with increasing temperature (Table 1). Because Fe is partitioned into the melt relative to coexisting olivine, an increase of Mg# in the olivine is an indicator of partial melting. In some experimental products, we did not observe any dendritic texture, although the Mg# of olivine had higher values than those of lower temperature runs. In those cases, we

---

T. Kawamoto, Department of Geology, Arizona State University, Tempe, AZ 85287, USA.
J. R. Holloway, Departments of Geology and Chemistry, Arizona State University, Tempe, AZ 85287, USA.

---

*To whom correspondence should be addressed. E-mail: john.holloway@asu.edu